



Cite this: RSC Adv., 2015, 5, 87713

Titanium aminophosphates: synthesis, characterization, antimicrobial and cytotoxicity studies†

Anumula Rajini, Ajay Kumar Adepu, Suman Chirra and Narayanan Venkatathri*

Titanium aminophosphates were prepared using titanium tetraisopropoxide, phosphoric acid and aliphatic amines. The synthesized TNPAP, TNOAP and TNDDAP aminophosphates were characterized by various physicochemical techniques. Powder XRD spectra of titanium aminophosphates suggest the presence of a $-Ti-O-$ phase. The % of titanium incorporated into the frameworks of titanium aminophosphates has been confirmed by EDAX analysis. The infrared and Raman spectra infer the presence of peaks due to vibrational bands of $Ti-O$, $P-O$, $Ti-N$, and $P-N$ as well as $Ti-O-P$, and $Ti-N-P$ linkages. The UV-Vis diffuse reflectance spectra reveal the presence of tetrahedral coordination of Ti in the framework. The XPS spectra suggest the presence of a $-O-Ti-N-$ or $-Ti-N-O-$ framework in TNPAP. The ^{31}P MASNMR spectra of titanium aminophosphates indicate the presence of two environmentally different tetrahedrally co-ordinated phosphorous atoms in the TNPAP framework, while other titanium aminophosphates have unique phosphorous atoms in the framework. The TNPAP, TNOAP and TNDDAP were evaluated for biological applications. TNDDAP only exhibits antimicrobial and nematicidal activity against *M. incognita* at higher concentrations and incubation time. TNPAP and TNDDAP show λ DNA cleavage activity while TNOAP does not. The *in vitro* anticancer activity has been studied using human cancer cell lines. TNPAP and TNOAP show anticancer activity only on the HL60 cell line. TNDDAP shows higher anticancer activity on HeLa and MCF7 cell lines and moderately on the HL60 cell line.

Received 29th July 2015
 Accepted 23rd September 2015
 DOI: 10.1039/c5ra15084a
www.rsc.org/advances

Introduction

Titanium is one of the best biomaterials known today.¹ It is one of the earliest transition metals to be investigated for its antitumor properties. Seventy-six percent of all titanium compounds that have been screened for their anticancer activity are derivatives of bis(β -diketonate)titanium(IV) complexes.² Bis(β -diketonate)titanium(IV) complexes are analogues of the titanium drug budotitane *cis*-diethoxybis(1-phenylbutane-1,3-dionato)titanium(IV).³

Recent advancements in titanium antitumor research have opened multiple directions to yield a more specific, stable to hydrolysis and improved anti-proliferative profile. Ti(IV) can bind to either the negatively charged phosphate on the backbone of DNA or to the base nitrogen donors.⁴

Phosphate based materials are important in several industrial acid catalysed reactions.⁵ In recent years inorganic phosphorous containing materials have received much attention on account of their ability to selectively uptake specific ions, resistance to oxidation, and their high thermal and chemical stability. In addition, the presence of phosphate in the

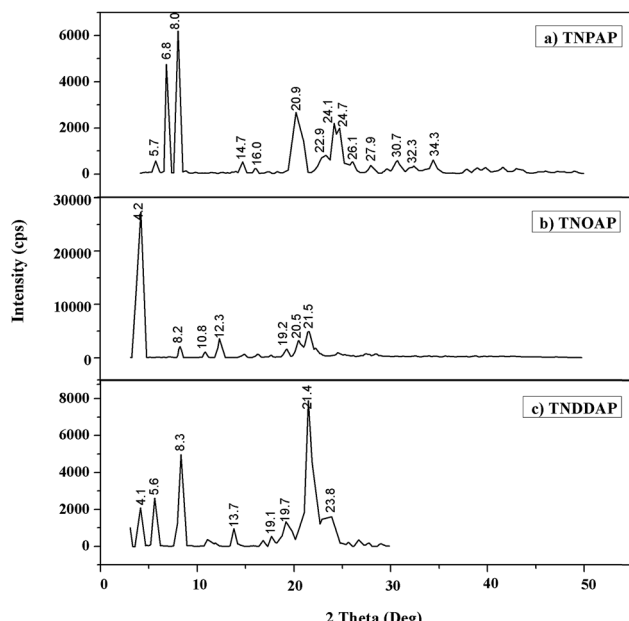


Fig. 1 Low and wide angle powder X-ray diffraction patterns of (a) TNPAP, (b) TNOAP and (c) TNDDAP.

Department of Chemistry, National Institute of Technology, Warangal 506 004, Telangana, India. E-mail: venkatathrin@yahoo.com; Tel: +91-9491319976

† Electronic supplementary information (ESI) available. See DOI: [10.1039/c5ra15084a](https://doi.org/10.1039/c5ra15084a)

materials seems to enhance the catalytic properties, stabilize the surface area and crystal phase, improve the surface acidity and make the material porous.⁶

Research on phosphate based materials with open frameworks is currently in progress due to their applications in catalysis and gas separation.⁷ The study of phosphates of transition metals has received great attention in recent years. Phosphate frameworks stabilize reduced oxidation states, due to their high charge (PO_4^{3-}) and hence favour the formation of anionic frameworks with a high degree of chemical, mechanical and thermal stability.

Aminophosphates are amine and phosphorous based materials. The organic functionality in the aminophosphate framework enhances hydrophobicity and shows high activity in base catalyzed reactions.⁸ Incorporation of transition metals such as titanium, palladium or vanadium in aminophosphates leads to novel materials with redox properties. In particular, a titanium cation Ti^{4+} in the framework position is found to exhibit good activity in shape selective redox reactions. The

materials were also evaluated for biological applications such as antimicrobial, nematicidal, DNA cleavage and anticancer activities. Titanium compounds are known for their antimicrobial and cytotoxicity properties. From our earlier report, we came to know that palladium aminophosphates also have the same property due to the modified electronic environment around palladium.⁹ This led us to extend these studies for titanium aminophosphates. We have observed better results using these compounds. These compounds are also economic, non-toxic and easy to synthesize compared to the previous ones. Furthermore, the characterization results show the morphology, porosity, co-ordination, oxidation state, insertion of titanium over the aminophosphate framework and the basic structure of all the synthesized compounds in the present study.

Experimental

Synthesis of titanium aminophosphates was carried out at room temperature. In a typical synthesis *n*-propyl amine (10.9 mL), *n*-

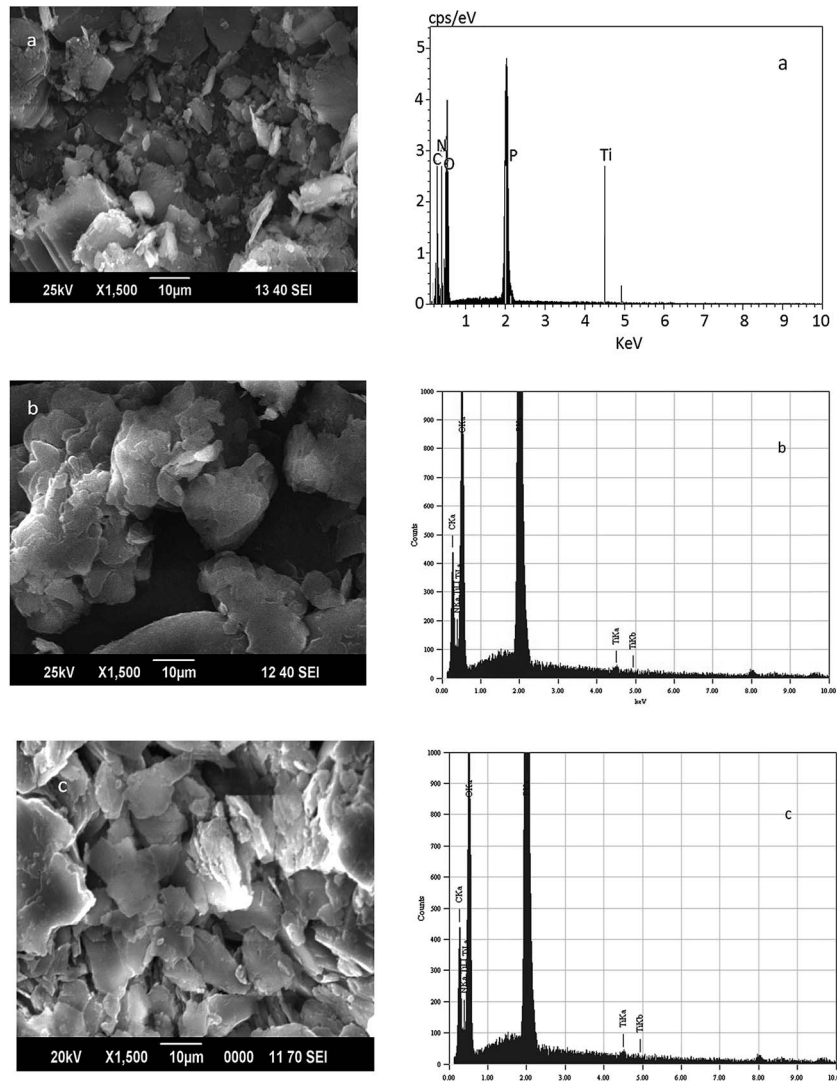


Fig. 2 Scanning electron microscopy-energy dispersive X-ray analyses of (a) TNPAP, (b) TNOAP and (c) TNDDAP.

octyl amine (22.0 mL) or *n*-dodecyl amine (30.6 mL) was added to 0.05 mL of titanium tetraisopropoxide and stirred. To this mixture, 1.87 mL of orthophosphoric acid was added and stirred vigorously to yield solid products (0.02 TiO₂ : P₂O₅ : 8 RNH₂). The products thus obtained were thoroughly washed with ether, dried at 40 °C for about 30 min and ground to a fine powder to obtain the respective titanium aminophosphates.

Qualitative phase analysis of titanium aminophosphate has been studied using a Bruker AXS D8 Advance diffractometer at room temperature with a Cu-K α X-ray source of wavelength 1.5406 Å using a Si (Li) PSD detector. The morphology and surface elemental composition of the material was investigated using scanning electron microscopy (SEM-EDAX) on a JEOL Model JSM-6390LV. Fourier transform infrared spectroscopy (FT-IR) was recorded on a Thermo Nicolet, Avatar 370 spectrophotometer equipped with a pyroelectric detector (DTGS type); a resolution of 4 cm⁻¹ was adopted and provided using a KBr beam splitter. Dispersive Raman spectroscopy was performed on a Bruker senterra at a wavelength of 532 nm using laser radiation as the source. The coordination and oxidation state of titanium in titanium aminophosphates were examined by a diffuse reflectance UV-Visible spectrophotometer (UV-Vis DRS) on a Varian Cary 5000 in the wavelength range of 175–800 nm. X-ray photoelectron spectroscopic analysis was carried out using an ESCA-3000 (VG Scientific, UK) instrument. ³¹P magic-angle spinning (MAS) nuclear magnetic resonance (NMR) spectroscopy was performed at room temperature on a Bruker DRX-500 AV-III 500(S) spectrometer, with a spinning

rate of 10–12 kHz operating at 121.49 MHz using a 5 mm dual probe. ¹³C cross polarization magic-angle spinning (CP-MAS) nuclear magnetic resonance (NMR) spectroscopy was performed at room temperature on a DSX-300 Avance-III 400(L) NMR spectrometer with a spinning rate of 10–12 kHz operating at 75.47 MHz using a 5 mm dual probe.

Results and discussion

Powder X-ray diffraction patterns of titanium *n*-propylamino phosphate (TNPAP), titanium *n*-octylaminophosphate (TNOAP) and titanium *n*-dodecylaminophosphate (TNDDAP) are shown in Fig. 1. TNPAP exhibits peaks at 2 θ degrees of 22.9°, 24.1°, 26.1°, 27.9° and 30.7° indicating the presence of a -Ti-O-linkage.²⁰ Similarly, the X-ray diffraction patterns of TNOAP and TNDDAP show peaks at 2 θ degrees of 5.6°, 8.2°, 8.3°, 13.7° and 18.7° corresponding to the presence of -Ti-O- with a mesoporous structure.^{10–12} TNOAP and TNDDAP exhibit low angle diffraction peaks at 4.1° and 4.2° characteristic of a mesoporous structure.

The SEM-EDAX images of TNPAP, TNOAP and TNDDAP are shown in Fig. 2. The SEM images of TNPAP and TNOAP reveal

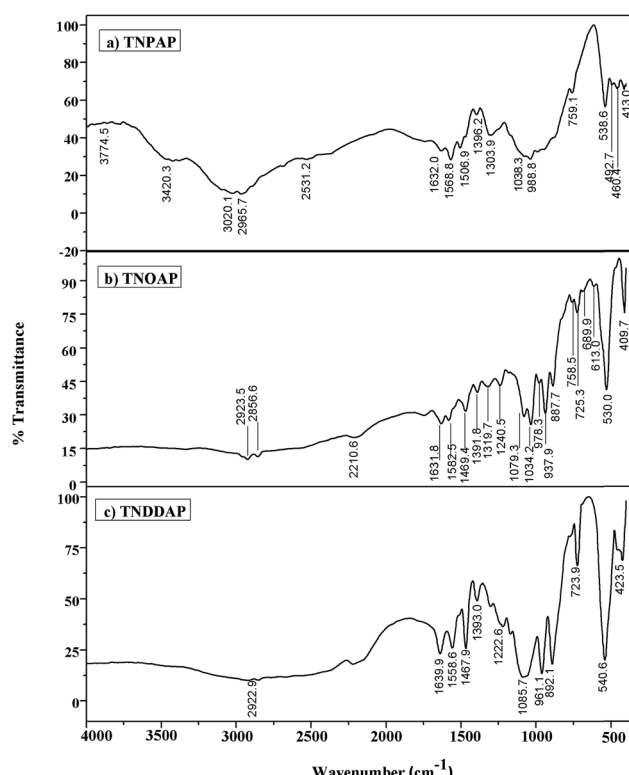


Fig. 3 Fourier transform infrared spectra of (a) TNPAP, (b) TNOAP and (c) TNDDAP.

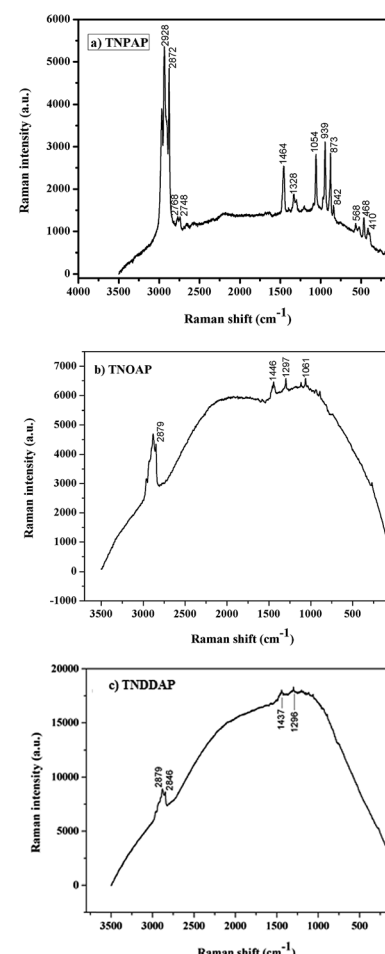


Fig. 4 Dispersive Raman spectra of (a) TNPAP, (b) TNOAP and (c) TNDDAP.

that the materials possess micron sized irregular flakes throughout the surface of the materials. The SEM image of TNDDAP shows that the material has a tubular like morphology. The EDAX analyses of TNPAP, TNOAP and TNDDAP show the distribution of the constituent elements O, P, N and Ti.

The thermogravimetry/differential thermal analyses of TNPAP, TNOAP and TNDDAP exhibit continuous weight loss up to 400 °C. This may be due to the removal of polymerized molecules. Thereafter, the weight remains constant which indicates the decomposition, combustion and crystallization of the organic material present in these materials. DTA shows exothermic peaks for the oxidative decomposition of organics and endothermic peaks due to dehydration and evaporation of the organic components.

The BET surface area analyses of titanium aminophosphates showed 60, 80 and 100 m² g⁻¹ of surface area for TNPAP, TNOAP and TNDDAP respectively. The decreased surface area compared to that reported for zeolites is due to the blockage of pores by alkyl groups present in amines.

The FT-IR spectra of TNPAP, TNOAP and TNDDAP are shown in Fig. 3. TNPAP shows a broad absorption band at 3420 cm⁻¹, which corresponds to O-H or N-H stretching vibrations. The peaks in the range of 3020–2850 cm⁻¹ correspond to alkyl symmetrical and asymmetrical stretching vibrations of amine groups in titanium aminophosphates.¹³ Peaks in the range of 1640–1630 cm⁻¹ are attributed to O-H bending vibrations of adsorbed water in titanium aminophosphates. Peaks observed at 1469 and 1467 cm⁻¹ are due to asymmetric deformation vibrations of alkyl groups in TNOAP and TNDDAP.¹⁴ The bands at 1079 and 1085 cm⁻¹ in TNOAP and TNDDAP are attributed to P-O stretching vibrations.^{15,16} The bands at 1038 and 1034 cm⁻¹ in TNPAP and TNOAP are due to Ti-O-P stretching vibrations. The bands around 980 cm⁻¹ are attributed to vibrational frequencies of the P-O group in titanium aminophosphates.¹⁶ Peaks at 1240 and 1222 cm⁻¹ in TNOAP and TNDDAP correspond to the characteristic absorbance of C-N bonds.¹⁷ The peaks at 887 and 892 cm⁻¹ in TNOAP and TNDDAP are due to asymmetric stretching vibrations of P-O-P groups. The peaks at 759 and 758 cm⁻¹ in TNPAP and TNOAP are attributed to non-bridging Ti-O bond vibrations.^{18,19} The peaks at about 725 and 723 cm⁻¹ in TNOAP and TNDDAP are assigned to symmetric stretching vibrations of P-O-P groups. The peaks in the range of 700–400 cm⁻¹ are attributed Ti-O and Ti-O-Ti vibrations in titanium aminophosphates. The peaks at 538, 492, 530 and 540 cm⁻¹ in titanium aminophosphates are attributed to P-O bending vibrations.^{20,21}

The Raman spectra of TNPAP, TNOAP and TNDDAP are shown in Fig. 4. Small peaks at 568 cm⁻¹ and 939 cm⁻¹ in TNPAP correspond to the stretching vibration of the Ti-O bond.^{22,23} The band at 1200 cm⁻¹ in TNPAP is associated with the asymmetric stretching vibration of the P-O bond of the phosphate group.²⁴

The UV-Visible diffuse reflectance spectra of TNPAP, TNOAP and TNDDAP are shown in Fig. 5. TNPAP and TNDDAP show peaks around 215 nm due to charge transfer transitions between the empty 3d-orbitals of Ti(IV) cations and 2p-orbitals of oxygen anions (O²⁻). The charge transfer transition infers

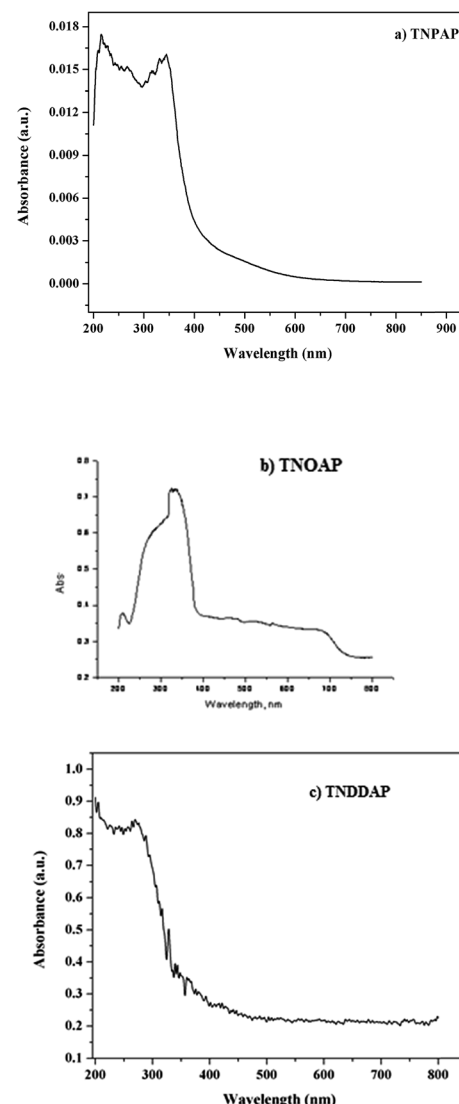


Fig. 5 Ultraviolet-Vis DR spectra of (a) TNPAP, (b) TNOAP and (c) TNDDAP.

the presence of titanium in tetrahedral coordination. TNPAP, TNOAP and TNDDAP show peaks at 343 and 325 nm respectively. These can be attributed to the existence of titanium in tetrahedral coordination.^{25,26}

The X-ray photoelectron spectroscopy (XPS) spectra of carbon, oxygen, nitrogen, phosphorous and titanium ions are shown in Fig. 6. In the XPS spectra of TNPAP, carbon 1s shows a peak at 288.0 eV. This can be attributed to carbon binding to oxygen, nitrogen and hydrogen respectively.²⁷ The peak around 534.0 eV corresponds to the oxygen 1s binding energy. This is due to the chemisorbed water and weakly adsorbed oxygen molecules on the surface. The binding energies of 534.2 eV and 532.4 eV are ascribed to oxygen co-contribution from Ti-O and P-O.²⁸ The peaks at 462 and 468 eV correspond to the binding energies of Ti 2p_{3/2} and 2p_{1/2} electrons, which is due to nitrogen doped interstitially into the titania matrix.²⁹ The higher binding energy value of titanium is due to a different electronic interaction with nitrogen compared to oxygen. They suggest a considerable

modification of the lattice due to N substitution. Titanium binds to nitrogen or oxygen atoms in the lattice to form O-Ti-N or Ti-N-O.²⁸ The P 2p shows a peak at 136.0 eV corresponding to the presence of phosphorous oxide (P_2O_5) in the TNPAP.²⁴

The ^{31}P MASNMR spectra of TNPAP, TNOAP and TNDDAP are shown in Fig. 7. TNPAP shows peaks at 4.654 ppm and -0.73 ppm with its side bands. The peaks are in 1 : 3 intensity ratios and suggest the existence of two crystallographically non-equivalent phosphorous atoms. The ^{31}P MASNMR spectra of TNOAP and TNDDAP show peaks at 5.824 and 1.924 ppm. The

presence of only one peak in TNOAP and TNDDAP spectra indicates that there is a unique chemical environment of phosphorous atoms. The ^{31}P peaks in the range of -5 to 3 ppm correspond to the presence of the mesoporous crystalline titanium phosphate framework in titanium aminophosphates.³⁰

The ^{13}C MASNMR spectra of TNPAP, TNOAP and TNDDAP are shown in Fig. 8. They show peaks at 41.12 and 39.80 ppm, which correspond to the C₁carbon bonded to the nitrogen atom of the amine group. The peaks at 34.46 and 32.12 ppm in TNOAP can be assigned to the C₂ and C₃ carbons linked to C₁

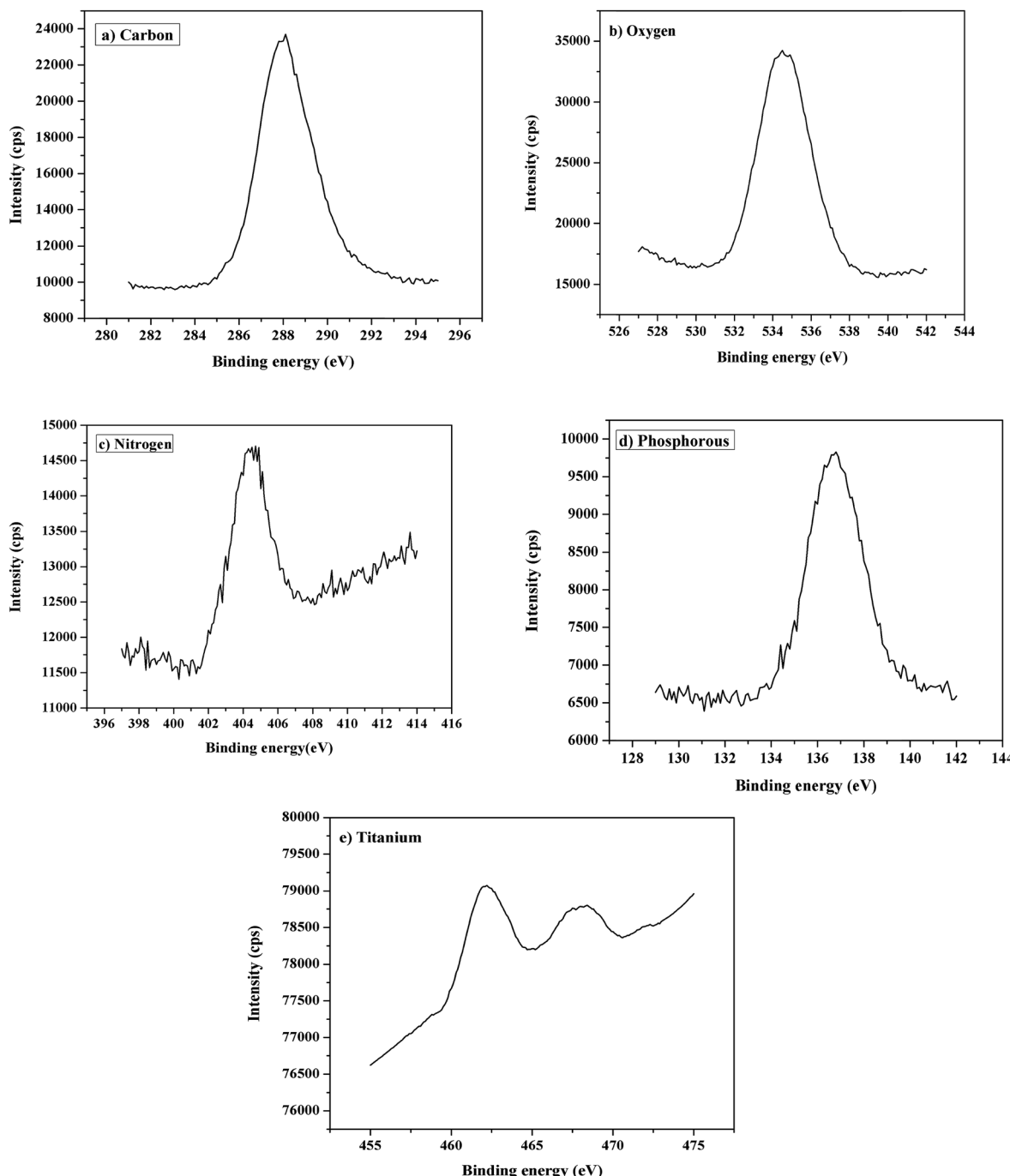


Fig. 6 X-ray photoelectron spectra of (a) carbon, (b) oxygen, (c) nitrogen, (d) phosphorous and (e) titanium ions in TNPAP.

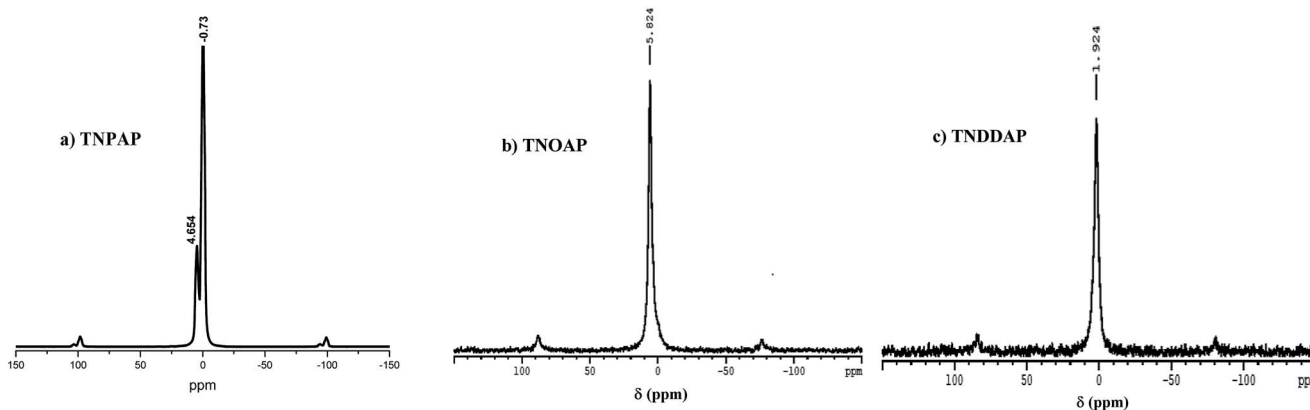


Fig. 7 ^{31}P magic angle spinning nuclear magnetic resonance spectra of (a) TNPAP, (b) TNOAP and (c) TNDDAP.

carbon which is directly attached to nitrogen of the amine group. The peak at 21.47 ppm in TNPAP can be assigned to the carbon of the methylene ($-\text{CH}_2-$) group. The peaks at 29.93, 28.37 and 24.49 ppm in TNOAP can be assigned to the carbons of the methylene ($-\text{CH}_2-$) groups. Peaks at 12.30 and 14.98 ppm in TNPAP and TNOAP can be attributed to the carbon of the terminal $-\text{CH}_3$ group of amine molecules.^{14,31}

Based on the above characterization, we have proposed the following plausible mechanism for titanium aminophosphate synthesis and the basic structure of the catalysts (Fig. 9). This is a trifunctional catalyst due to the presence of titanium ion (redox), amine (Lewis base) and exchangeable proton (acid) sites. As the reaction is carried out in a solvent free condition, there is no residue from the synthesis of the catalyst (it means 100% yield). So all the inputted titanium and amine are present in the basic structure. The presence of solid acid sites are deduced from the proposed structure, which is confirmed by the NaCl ion exchange experiment.

The titanium aminophosphates were evaluated for their *in vitro* antimicrobial activity. The minimum inhibitory concentrations (MICs) for the antimicrobial activity of titanium aminophosphates are presented in Table 1. The results reveal that TNPAP and TNOAP did not show any antimicrobial activity. The inactivity of TNPAP and TNOAP in antimicrobial activity is due to their low lipophilicity which makes the materials unable to penetrate through the lipid membrane. Hence the materials neither block nor inhibit the growth of the microorganism. TNDDAP exhibits less to moderate activity against all the microbial strains tested when compared with the standard antibiotics ampicillin and clotrimazole.

TNDDAP inhibits the growth of bacteria and the MIC values were found in the range of 14 to 26 $\mu\text{g mL}^{-1}$. The TNDDAP exhibits the maximum anti-bacterial activity against *S. aureus* with a MIC value of 14 $\mu\text{g mL}^{-1}$ and moderate against *P. fluorescens* with a MIC value of 26 $\mu\text{g mL}^{-1}$. The MIC value against *E. coli* was found to be 18 $\mu\text{g mL}^{-1}$. The anti-fungal activity of TNDDAP against *C. albicans* shows a MIC value of 16 $\mu\text{g mL}^{-1}$.

The variation in length of the alkyl chain of an amine is thought to influence the extent of antimicrobial activity.³² It is also reported in the literature that the antimicrobial activity

depends on the properties of the amine side chains.³³ The longer alkyl chain amine in TNDDAP shows higher antimicrobial activity than shorter chains in TNPAP and TNOAP.

The electron releasing groups of dodecylamine in TNDDAP reduces the polarity by partial sharing of its charge with the positive charge of the titanium ion.^{34,35} Furthermore, it increases the electron delocalization and stabilizes the whole framework and enhances the lipophilicity. The enhanced lipophilicity favours the penetration of materials into the lipid membranes of the bacterial cell more efficiently.^{36,37}

Furthermore, the activity of TNDDAP can also be explained on the basis of the overtones concept and the chelation theory.^{38,39} According to the overtones concept of cell permeability, the lipid membrane that surrounds the cell favors the passage of only lipid soluble materials. Liposolubility is an important factor which controls the antimicrobial activity. The activity is due to the lipophilic nature of the material arising from chelation.⁴⁰

The nematicidal activity of titanium aminophosphates was evaluated against *Meloidogyne incognita* with different concentrations after 24 and 48 h of incubation time and the results are presented in Table 2.

The results reveal that, TNPAP and TNOAP did not show any activity. TNDDAP exhibits 78% mortality at a concentration of 250 $\mu\text{g mL}^{-1}$ after 48 h exposure indicating good activity. Aliphatic amines having a carbon chain length of 9 to 35 are found to be highly lethal to nematodes and parasites.⁴¹ However, the activity of TNDDAP depends on concentration and time *i.e.*, the activity was higher at high concentrations and was found to increase with incubation time. The percentage mortality in the presence of TNDDAP was increased from 18 to 78% with an increase in the concentration from 50 to 250 $\mu\text{g mL}^{-1}$ and incubation time from 24 to 48 h.

The DNA cleavage activity of titanium aminophosphates was investigated using agarose gel electrophoresis on λ DNA. The gel electrophoresis image of titanium aminophosphates is shown in Fig. 10. Control DNA (in the figure, lane labelled as C) does not show any cleavage of DNA in its lane. FeSO_4 (in the figure, lane labelled as +ve) was used as a standard, and the complete disappearance of bands was observed in its lane, indicating

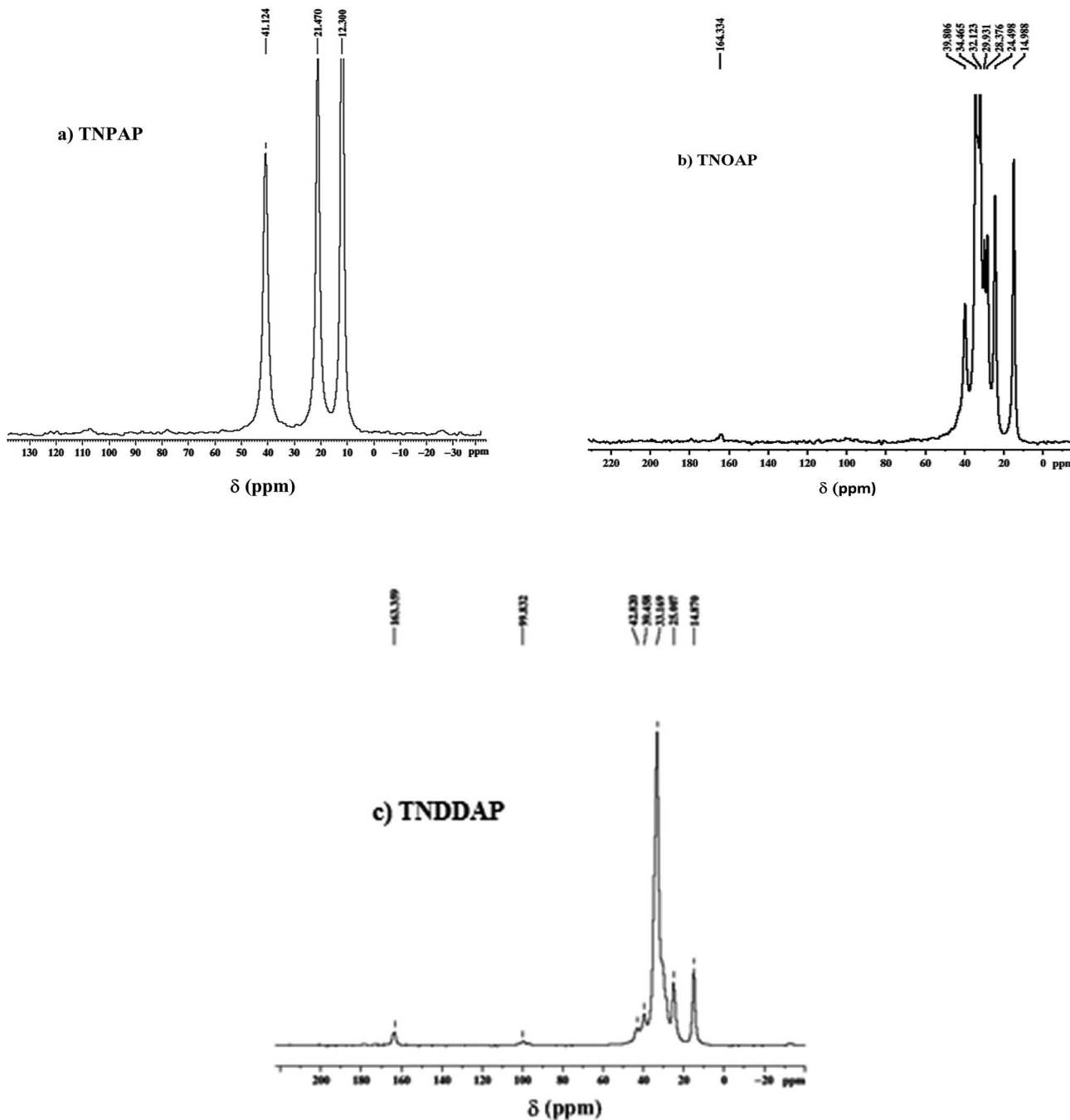


Fig. 8 ^{13}C magic angle spinning nuclear magnetic resonance spectra of (a) TNPAP, (b) TNOAP and (c) TNDDAP.

DNA cleavage. The lanes TNPAP and TNDDAP clearly show the complete disappearance of control bands. Lane TNOAP does not show any DNA cleavage. It indicates that the titanium aminophosphates exhibit significant DNA cleavage without using any external reagents like H_2O_2 . The DNA cleavage activity of titanium aminophosphates may be due to the electrostatic interactions of titanium with the base pairs of the λ DNA molecule.

Synthesized titanium aminophosphates TNPAP, TNOAP and TNDDAP were evaluated for *in vitro* anticancer activity against human cancer cell lines such as MCF7, HeLa and HL60 by the

sulforhodamine B assay. The growth inhibition of 50% (GI50) values for TNPAP, TNOAP, TNDDAP and the standard drug doxorubicin obtained against selected cancer cell lines are shown in Table 3.

Estimation based on the GI50 values shows that all the titanium aminophosphates exhibit anticancer activity. TNPAP and TNOAP exhibit activity exclusively on the HL60 cell line with GI50 values of 12.7 and $48.3 \mu\text{g mL}^{-1}$. All three materials have no effect on the viability of HeLa and MCF7 cell lines. The low anticancer activity of TNPAP and TNOAP is due to their low solubility or they are not taken up by the cell lines.⁴² Among the

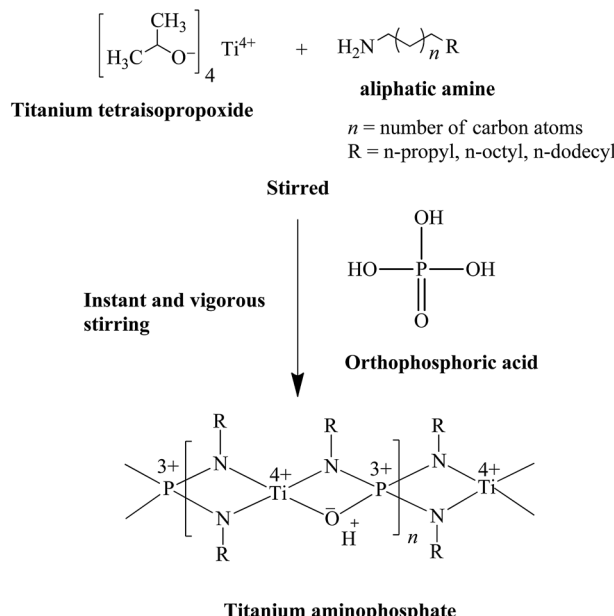


Fig. 9 Schematic synthesis mechanism and proposed basic structure of titanium aminophosphate.

Table 1 Minimum inhibitory concentration values ($\mu\text{g mL}^{-1}$) for the antimicrobial activity of titanium aminophosphates

Compound	<i>B. subtilis</i>	<i>S. aureus</i>	<i>P. vulgaris</i>	<i>P. fluorescens</i>	<i>E. coli</i>	<i>C. albicans</i>
TNPAP	—	—	—	—	—	—
TNOAP	—	—	—	—	—	—
TNDDAP	16	14	22	26	18	16
Ampicillin	14	12	16	16	16	—
Clotrimazole	—	—	—	—	—	10

Table 2 Nematicidal activity (% mortality) observed using different concentrations of titanium aminophosphates against *Meloidogyne incognita*. Effect of the incubation time on % mortality

Compound	24 h			48 h		
	250	150	50	250	150	50
TNPAP	—	—	—	—	—	—
TNOAP	—	—	—	—	—	—
TNDDAP	44	32	18	78	63	40

three compounds tested, TNDDAP exhibits higher anticancer activity on HeLa (Fig. 11a) and MCF7 (Fig. 11b) cell lines with GI₅₀ values of $10.6 \mu\text{g mL}^{-1}$ and $13.2 \mu\text{g mL}^{-1}$ and moderate activity on the HL60 cell line (Fig. 11c) with a GI₅₀ value of $39.8 \mu\text{g mL}^{-1}$.

The anticancer activity of the titanium aminophosphates depends on lipophilicity and membrane permeability because they have to cross the hydrophobic cell membrane to exhibit their activity. Previous studies on pharmacokinetics revealed

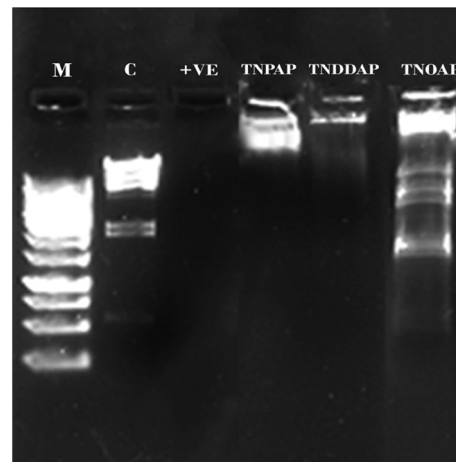


Fig. 10 Gel electrophoresis image of titanium aminophosphates. DNA cleavage activity of titanium aminophosphates against λ DNA: M, DNA + marker; lane C, DNA alone; lane +ve, DNA + FeSO_4 ; lane TNPAP, DNA + TNPAP; lane TNDDAP, DNA + TNDDAP; lane TNOAP, DNA + TNOAP.

Table 3 Anticancer activity of titanium aminophosphates on human HeLa, MCF7 and HL60 cancer cell lines using sulforhodamine B assay^a

Cell lines	GI ₅₀		GI ₅₀		GI ₅₀	
	TNPAP	Doxorubicin	TNOAP	Doxorubicin	TNDDAP	Doxorubicin
HeLa	>80	<10	>80	<10	10.6	<10
MCF7	>80	<10	>80	<10	13.2	<10
HL60	12.7	<10	48.3	<10	39.8	<10

^a Note: GI₅₀ (μM) = growth inhibition of 50% (GI₅₀), which is the drug concentration resulting in a 50% reduction in the net protein increase, doxorubicin = positive control compound, HeLa = cervix, MCF7 = breast and HL60 = leukemia cancer cell lines.

that the lipophilicity of the compounds increases as the carbon chain length increases. Increased lipophilicity leads to better permeability through the cell membrane and results in an increased potency.^{43,44} The TNDDAP with 12 carbon alkyl chains has higher lipophilicity and passes rapidly through a permeable membrane compared to the 3 and 8 carbon atoms contained within TNPAP and TNOAP. Consequently TNDDAP exhibits the highest anticancer activity. These results clearly indicate that the length of the alkyl chain in the amine plays an important role in determining the anticancer activity of titanium aminophosphates. It was observed that the length of the alkyl chain coordinated to the titanium is a significant factor which influences the toxicity of the compounds.

The anticancer activity of titanium aminophosphates can be understood due to following reasons. The high oxidation state of Ti(IV) in titanium aminophosphates may prevent oxidation in the body. The open framework, and neutral charge on the titanium aminophosphates allow the passive diffusion of titanium ions into cancer cells. The presence of amino groups in titanium aminophosphates also influences the anticancer activity. Results indicate that the compounds should possess at

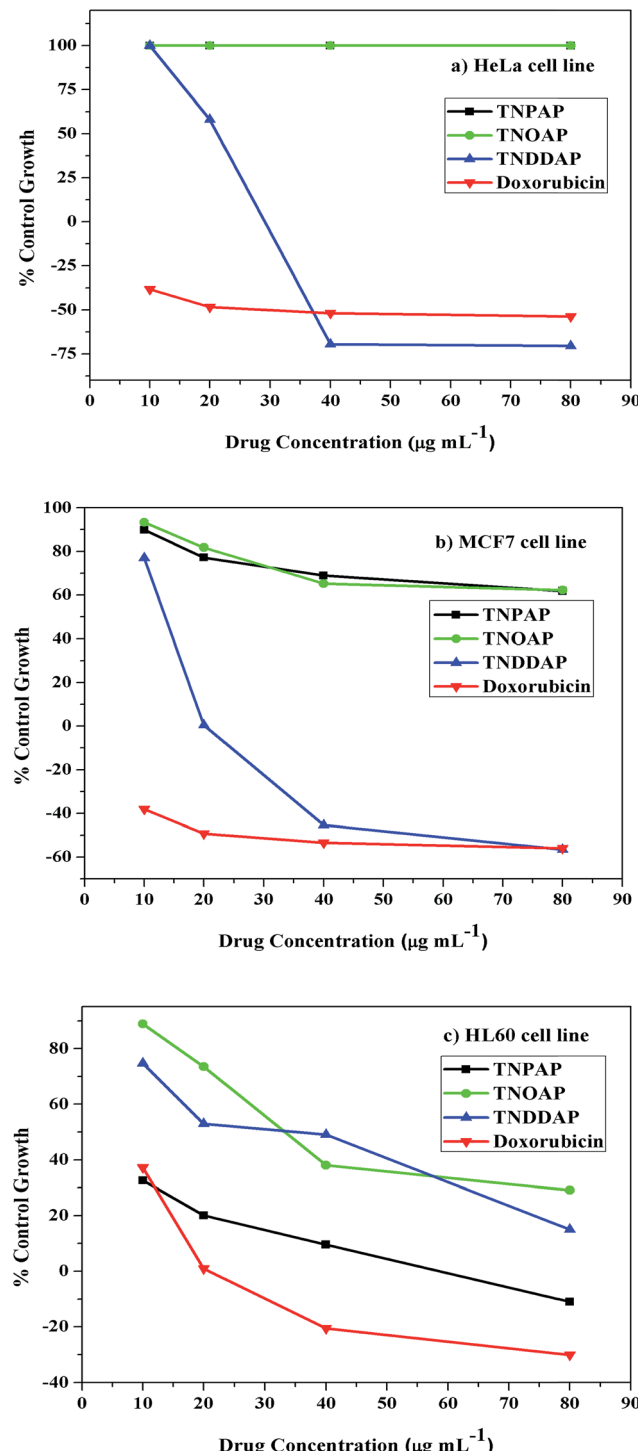


Fig. 11 Anticancer activity of titanium aminophosphates on human cancer cell lines (a) HeLa, (b) MCF7 and (c) HL60 using the sulforhodamine B assay.

least one N–H bond linkage in order to exhibit anticancer activity.

Amino groups in titanium aminophosphates may increase the electron density on the Ti(IV) centre, stabilize it and enhance its interaction with the Lewis base sites of DNA.⁴⁷ Previous studies on anticancer activity reported that titanium ions may

intercalate with DNA base pairs and allow for titanium–DNA interactions. This results in passive diffusion of titanium ions into the cancer cells and shows anticancer activity.⁴⁵ These studies indicate that the titanium aminophosphates bind strongly to the phosphate groups of nucleotides and lead to anticancer activity.⁴⁶ This may be due to a higher efficiency of bonding of titanium to phosphorus.

Conclusions

Titanium aminophosphates were prepared by employing titanium tetraisopropoxide, phosphoric acid and aliphatic amines. The synthesized TNPAP, TNOAP and TNDDAP aminophosphates were characterized by various physicochemical techniques. Powder XRD spectra of titanium aminophosphates suggest the presence of a -Ti–O- phase. The % of titanium incorporated into the frameworks of titanium aminophosphates has been confirmed by EDAX analysis. The infrared and Raman spectra infer the presence of peaks due to vibrational bands of Ti–O, P–O and Ti–O–P linkages. The UV-Vis diffuse reflectance spectra reveal the presence of tetrahedral coordination of Ti in the framework. The XPS spectra suggest the presence of -O–Ti–N- or -Ti–N–O- framework in TNPAP. The ³¹P MASNMR spectra of titanium aminophosphates indicate the presence of crystalline titanium phosphate framework. The TNPAP, TNOAP and TNDDAP were evaluated for biological applications. TNDDAP only exhibits antimicrobial and nematicidal activity against *M. incognita* at higher concentrations and incubation time. TNPAP and TNDDAP show λDNA cleavage activity except TNOAP. The *in vitro* anticancer activity has been studied on human cancer cell lines. The TNPAP and TNOAP show anticancer activity only on the HL60 cell line. TNDDAP shows higher anticancer activity against HeLa and MCF7 cell lines and moderately on the HL60 cell line.

Acknowledgements

The authors A. R., A. A. K. and S. C. thank MHRD, New Delhi for a research fellowship.

References

- 1 S. Rafique, M. Idrees, A. Nasim, H. Akbar and A. Athar, *Biotechnol. Mol. Biol. Rev.*, 2010, **5**, 38.
- 2 R. Huang, A. Wallqvist and D. G. Covell, *Biochem. Pharmacol.*, 2005, **69**, 1009.
- 3 B. K. Keppler, C. Friesen, H. Vongerichten and E. Vogel, *Met. Complexes Cancer Chemother.*, 1993, 297.
- 4 H. Z. Sun, H. Y. Li and P. J. Sadler, *Chem. Rev.*, 1999, **99**, 2817.
- 5 S. K. Samantaray, T. Mishra and K. M. Parida, *J. Mol. Catal. A: Chem.*, 2000, **156**, 267.
- 6 S. K. Samantaray and K. M. Parida, *J. Mol. Catal. A: Chem.*, 2001, **176**, 151.
- 7 A. K. Cheetham, G. Ferey and T. Loiseau, *Angew. Chem., Int. Ed.*, 1999, **38**, 3268.
- 8 C. Berlini, M. Guidotti, G. Moretti, R. Psaro and N. Ravasio, *Catal. Today*, 2000, **60**, 219.

9 A. Rajini, A. Ajay kumar, S. Chirra and N. Venkatathri, *RSC Adv.*, 2015, **5**, 66956.

10 K. Khosravi, M. E. Hoque, B. Dimock, H. Hintelmann and C. D. Metcalfe, *Anal. Chim. Acta*, 2012, **713**, 86.

11 D. M. Antonelli and J. Y. Ying, *Angew. Chem., Int. Ed.*, 1995, **34**, 2014.

12 A. R. Khataee and M. B. Kasiri, *J. Mol. Catal. A: Chem.*, 2010, **328**, 8.

13 M. Nagao and Y. Suda, *Langmuir*, 1989, **5**, 42.

14 L. Zhang, J. Xu, G. Hou, H. Tang and F. Deng, *J. Colloid Interface Sci.*, 2007, **311**, 38.

15 K. M. Parida, M. Acharya, S. K. Samantaray and T. Mishra, *J. Colloid Interface Sci.*, 1999, **217**, 388.

16 S. F. Lincoln and D. R. Stranks, *Aust. J. Chem.*, 1968, **21**, 37.

17 X. A. Zhao, C. W. Ong, Y. C. Tsang, Y. W. Wong, P. W. Chan and C. L. Choy, *Appl. Phys. Lett.*, 1995, **66**, 2652.

18 S. Sakka, F. Miyaji and K. Fukumi, *J. Non-Cryst. Solids*, 1989, **112**, 64.

19 N. G. Chernorukov, I. A. Korshunov and M. I. Zhuk, *Russ. J. Inorg. Chem.*, 1982, **27**, 1728.

20 A. Nilchi, M. G. Maragheh, A. Khanchi, M. A. Farajzadeh and A. A. Aghaei, *J. Radioanal. Nucl. Chem.*, 2004, **261**, 393.

21 B. B. Sahu and K. Parida, *J. Colloid Interface Sci.*, 2002, **248**, 221.

22 C. Schmutz, P. Barboux, F. Ribot, F. Taulelle, M. Verdaguier and C. Fernandez-Lorenzo, *J. Non-Cryst. Solids*, 1994, **170**, 250.

23 X. Gao and I. E. Wachs, *Catal. Today*, 1999, **51**, 233.

24 L. A. Farrow and E. M. Vogel, *J. Non-Cryst. Solids*, 1992, **143**, 59.

25 S. Jhung, Y. S. Uh and H. Chon, *Appl. Catal.*, 1990, **62**, 61.

26 J. Kornatowski, B. Wichterlova, M. Roswadowski and W. H. Baur, *Stud. Surf. Sci. Catal.*, 1994, **84**, 117.

27 H.-F. Yu and S.-T. Yang, *J. Alloys Compd.*, 2010, **492**, 695.

28 K. M. Parida and N. Sahu, *J. Mol. Catal. A: Chem.*, 2008, **287**, 151.

29 C. Di Valentin, E. Finazzi, G. Pacchioni, A. Selloni, S. Livraghi, M. C. Paganini and E. Giamello, *Chem. Phys.*, 2007, **339**, 44.

30 E. Jaimez, A. Bortun, G. B. Hix, J. R. Garcia, J. Rodriguez and R. C. T. Slade, *J. Chem. Soc., Dalton Trans.*, 1996, 2285.

31 A. Hayashi, H. Nakayama and M. Tsuhako, *Solid State Sci.*, 2009, **11**, 1007.

32 A. M. Bonilla and M. F. Garcia, *Prog. Polym. Sci.*, 2012, **37**, 281.

33 B. Keshavan and H. Kempe Gowda, *Turk. J. Chem.*, 2002, **26**, 237.

34 K. Kralova, K. Kissova, O. Svajlenova and J. Vanco, *Chem. Pap.*, 2000, **58**, 357.

35 K. Shanker, R. Rohini, V. Ravinder, P. M. Reddy and Y. P. Ho, *Spectrochim. Acta, Part A*, 2009, **73**, 205.

36 N. M. A. Atabay, B. Dulger and F. Gucin, *Eur. J. Med. Chem.*, 2005, **40**, 1096.

37 B. G. Tweedy, *Phytopathology*, 1964, **55**, 910.

38 M. N. Patel, B. S. Bhatt and P. A. Dosi, *Z. Anorg. Allg. Chem.*, 2012, **638**, 152.

39 S. D. L. Yadav and S. Singh, *Indian J. Chem., Sect. B: Org. Chem. Incl. Med. Chem.*, 2001, **40**, 440.

40 M. J. Thompson, J. Feldmesser and W. E. Robbins, *US Pat.*, 4,036,987 A, 1977.

41 J. K. Seydel and K. J. Schaper, in *Pharmacokinetics: Theory and Methodology*, ed. M. Rowland and G. Tucker, Pergamon Press, New York, 1986, p. 311.

42 R. B. Silverman and M. W. Holladay, *The Organic Chemistry of Drug Design and Drug Action*, Academic Press, 3rd edn, 1992, p. 422.

43 S. Toon and M. Rowland, *J. Pharmacol. Exp. Ther.*, 1983, **225**, 752.

44 S. Gomez Ruiz, G. N. Kaluaderovic, S. Prashar, D. Polo-Ceron, M. Fajardo, Z. Zizak, T. J. Sabo and Z. D. Juranic, *J. Inorg. Biochem.*, 2008, **102**, 1558.

45 C. Pampillon, J. Claffey, K. Strohfeldt and M. Tacke, *Eur. J. Med. Chem.*, 2008, **43**, 122.

46 M. L. Guo, Z. J. Guo and P. J. Sadler, *J. Biol. Inorg. Chem.*, 2001, **6**, 698.

47 S. Gomez Ruiz, G. N. Kaluaderovic, S. Prashar, D. Polo-Ceron, M. Fajardo, Z. Zizak, T. J. Sabo and Z. D. Juranic, *J. Inorg. Biochem.*, 2008, **102**, 1558.